High-Speed Biped Walking Using Swinging-Arms Based on Principle of Up-and-Down Wobbling Mass

Yuta Hanazawa[1] and Fumihiko Asano[2]

Abstract— **In this paper, we present a speeding-up method for biped walking using swinging-arm motion based on the principle of an up-and-down wobbling mass. We have shown that biped robots with a wobbling mass can achieve fast walking using an active up-and-down motion of the wobbling mass. We have also shown the principle that the active up-and-down motion increases walking speed of biped robots. We apply this principle to a biped robot with two linked arm like humans for achieving high-speed limit cycle walking. We show that the proposed method achieves high-speed limit cycle walking for biped robots with arms.**

I. INTRODUCTION

Biped robot have high moving performance in various environments and we expect that they work in various field [1], [2], [3]. These biped robot fast and stable dynamic walking. However, energy-efficiency of the many biped robot is bad in dynamic walking and this problem degrades the usability of the biped robot. We have studied active dynamic walking based on the principle of passive dynamic walking [4]. This type walking is known as limit cycle walking and many limit cycle walkers have been proposed [5], [6], [7], [8], [9].

Limit cycle walkers achieve energy-efficient walking but their walking speed are typically slow. Speeding-up methods for limit cycle walkers have thus developed. Asano et al. have shown fast limit cycle walking using property of arc-feet [10]. They have also proposed high-speed limit cycle walking using principle of parametric excitation mechanism using telescoping legs [11]. Hobbelen et al. have developed speeding-up method using torso posture [12]. Hanazawa et al. have shown speeding-up method using ankle springs and inerters [9]. We have also proposed a speeding-up method for limit cycle waking using an active up-and-down control of a wobbling mass [13]. We have also shown a principle for the speeding-up biped walking by the wobbling mass method mathematically. This principle is a regular up-and-down wobbling mass according to the stance leg angle and the regular motion of the wobbling mass generates propulsive effects.

We consider that biped robots with arms achieving limit cycle walking work at various field in the future. We also expect that the biped robots with arms serve for many tasks using their arms instead of humans. We thus apply the principle of the up-and-down wobbling mass to biped robot with two linked arms for speeding-up limit cycle walking.

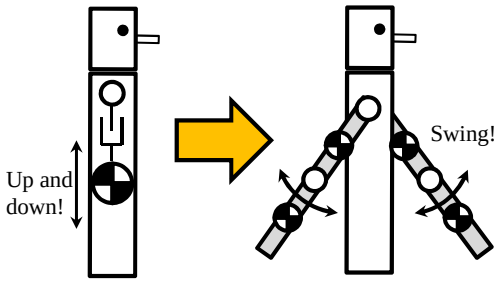

Fig. 1. Schematic illustration of analogy between up-and-down motion of wobbling mass and swinging-arms

In this paper, we propose a novel speeding-up method for biped robots using their arms based on the principle of the up-and-down wobbling mass. Fig. 1 shows schematic illustration of analogy between up-and-down motion of a wobbling mass and swinging-arms. We design control method for biped robot with arms from the viewpoint of this analogy. We show the validity of the proposed method through numerical simulations.

II. MODEL OF BIPED ROBOT

A. Dynamic equation

We use a model of a biped robot with two linked arms (Fig. 2). This robot also has six actuators for active control of the arms, the torso and the swing-leg (thigh). Dynamic equation of the robot is given by

$$\boldsymbol{M}(\boldsymbol{q})\ddot{\boldsymbol{q}} + \boldsymbol{H}(\boldsymbol{q}, \dot{\boldsymbol{q}}) = \boldsymbol{S}\boldsymbol{u} + \boldsymbol{J}_c(\boldsymbol{q})^{\mathrm{T}}\boldsymbol{\lambda}, \tag{1}$$

where $\boldsymbol{q} = [\theta_1,\ \theta_2,\ \theta_3,\ \theta_4,\ \theta_5,\ \theta_6,\ \theta_7,\ x_1,\ z_1]^{\mathrm{T}}$ is the generalized coordinate vector, $\boldsymbol{M}(\boldsymbol{q}) \in \mathbb{R}^{9\times 9}$ is the inertia matrix, $\boldsymbol{H}(\boldsymbol{q}, \dot{\boldsymbol{q}}) \in \mathbb{R}^9$ is the vector that consists of Coriolis, centrifugal force and gravitational vector, $\boldsymbol{u} = [u_1,\ u_2,\ u_3,\ u_4,\ u_5,\ u_6]^{\mathrm{T}}$ is the input vector, $\boldsymbol{S} \in \mathbb{R}^{9\times 6}$ is the driving matrix and is detailed as

$$\boldsymbol{S} = \begin{bmatrix} 0 & -1 & 0 & 0 & 0 & 0 \\ 1 & 0 & 0 & 0 & 0 & 0 \\ -1 & 1 & -1 & 0 & -1 & 0 \\ 0 & 0 & 1 & -1 & 0 & 0 \\ 0 & 0 & 0 & 1 & 0 & 0 \\ 0 & 0 & 0 & 0 & 1 & -1 \\ 0 & 0 & 0 & 0 & 0 & 1 \\ 0 & 0 & 0 & 0 & 0 & 0 \\ 0 & 0 & 0 & 0 & 0 & 0 \end{bmatrix}.$$

[1]Y. Hanazawa is with the Dept. of Applied Science for Integrated System Engineering, Graduate School of Engineering, Kyushu Institute of Technology, 1-1 Sensui, Tobata, Kitakyushu, Fukuoka 804-8550, JAPAN hanazawa-y@ise.kyutech.ac.jp [2]F. Asano is with the School of Information Science, Japan Advanced Institute of Science and Technology, 1-1 Asahidai, Nomi, Ishikawa 923-1292, JAPAN fasano@jaist.ac.jp

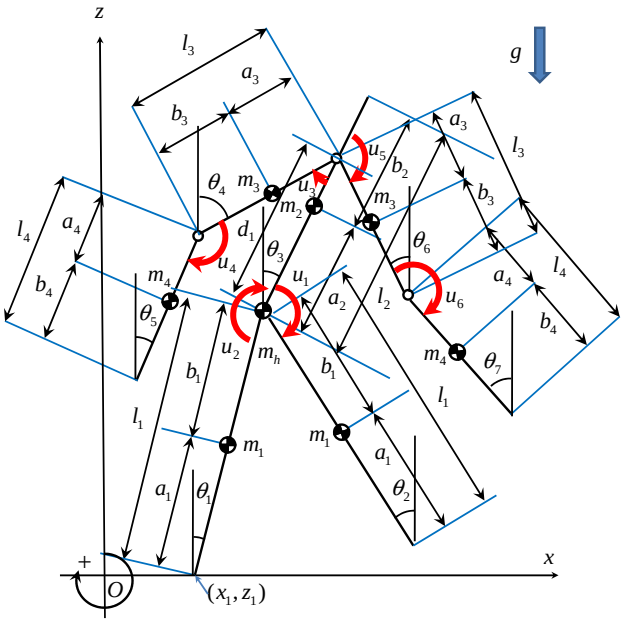

Fig. 2. Model of biped robot with two linked arms

$\boldsymbol{J}_c(\boldsymbol{q}) \in \mathbb{R}^{N\times 9}$ is the Jacobian matrix and is determined according to the constraint conditions of the robot and N is the number of constraint conditions. $\boldsymbol{\lambda} \in \mathbb{R}^N$ is the constraint force vector given by

$$\boldsymbol{\lambda} = -\boldsymbol{X}(\boldsymbol{q})^{-1}(\boldsymbol{J}_c(\boldsymbol{q})\boldsymbol{M}(\boldsymbol{q})^{-1}\boldsymbol{\Gamma}(\boldsymbol{q},\dot{\boldsymbol{q}},\boldsymbol{u}) + \dot{\boldsymbol{J}}_c(\boldsymbol{q},\dot{\boldsymbol{q}})\dot{\boldsymbol{q}}), \quad (2)$$

$$\boldsymbol{X}(\boldsymbol{q}) = \boldsymbol{J}_c(\boldsymbol{q})\boldsymbol{M}(\boldsymbol{q})^{-1}\boldsymbol{J}_c(\boldsymbol{q})^{\mathrm{T}}, \quad (3)$$

$$\boldsymbol{\Gamma}(\boldsymbol{q},\dot{\boldsymbol{q}},\boldsymbol{u}) = \boldsymbol{S}\boldsymbol{u} - \boldsymbol{H}(\boldsymbol{q},\dot{\boldsymbol{q}}). \quad (4)$$

Although the swing leg of the biped robot scuffs since the biped robot does not have knees, we ignore this foot-scuffing in the simulation.

B. Constraint conditions

Since the contact point of the biped robot is constrained with ground, constraint equations are expressed as

$$\dot{x}_1 = 0, \quad (5)$$

$$\dot{z}_1 = 0. \quad (6)$$

From these equations, we obtain $\boldsymbol{J}_c(\boldsymbol{q}) \in \mathbb{R}^{2\times 9}$ and $\dot{\boldsymbol{J}}_c(\boldsymbol{q},\dot{\boldsymbol{q}}) \in \mathbb{R}^{2\times 9}$ as

$$\boldsymbol{J}_c(\boldsymbol{q})\dot{\boldsymbol{q}} = \begin{bmatrix} 0 & 0 & 0 & 0 & 0 & 0 & 0 & 1 & 0 \\ 0 & 0 & 0 & 0 & 0 & 0 & 0 & 0 & 1 \end{bmatrix} \dot{\boldsymbol{q}} = \boldsymbol{0}_{2\times 1}, \quad (7)$$

$$\dot{\boldsymbol{J}}_c(\boldsymbol{q},\dot{\boldsymbol{q}}) = \boldsymbol{0}_{2\times 9} \quad (8)$$

C. Impact equation

We assume that the collision of the swing-leg with the ground is inelastic and instantaneous. We can derive the velocity immediately after impact by solving the impact equations described in the following [14]. Since the contact point of the biped robot is constrained with the ground at the collision of the swing-leg, constraint equations are expressed as

$$l_1\cos\theta_1\dot{\theta}_1 - l_2\cos\theta_2\dot{\theta}_2 + \dot{x}_1 = 0, \quad (9)$$

$$-l_1\sin\theta_1\dot{\theta}_1 + l_2\sin\theta_2\dot{\theta}_2 + \dot{z}_1 = 0. \quad (10)$$

From these equations, the instantaneous constraint matrix $\boldsymbol{J}_I(\boldsymbol{q}) \in \mathbb{R}^{2\times 9}$ is given by

$$\boldsymbol{J}_I(\boldsymbol{q}) = \begin{bmatrix} l_1\cos\theta_1 & -l_2\cos\theta_2 & 0 & 0 & 0 & 0 & 0 & 1 & 0 \\ -l_1\sin\theta_1 & l_2\sin\theta_2 & 0 & 0 & 0 & 0 & 0 & 0 & 1 \end{bmatrix}. \quad (11)$$

Impulsive force vector, $\boldsymbol{\lambda}_I \in \mathbb{R}^2$, and a velocity vector, $\dot{\boldsymbol{q}}^+ \in \mathbb{R}^9$, immediately after the impact are given by

$$\boldsymbol{\lambda}_I = -\boldsymbol{X}_I(\boldsymbol{q})^{-1}\boldsymbol{J}_I(\boldsymbol{q})\dot{\boldsymbol{q}}^-, \quad (12)$$

$$\boldsymbol{X}_I(\boldsymbol{q}) = \boldsymbol{J}_I(\boldsymbol{q})\boldsymbol{M}(\boldsymbol{q})^{-1}\boldsymbol{J}_I(\boldsymbol{q})^{\mathrm{T}}, \quad (13)$$

$$\dot{\boldsymbol{q}}^+ = (\boldsymbol{I} - \boldsymbol{M}(\boldsymbol{q})^{-1}\boldsymbol{J}_I(\boldsymbol{q})^{\mathrm{T}}\boldsymbol{X}_I(\boldsymbol{q})^{-1}\boldsymbol{J}_I(\boldsymbol{q}))\dot{\boldsymbol{q}}^-, \quad (14)$$

where $\dot{\boldsymbol{q}}^- \in \mathbb{R}^9$ is the velocity vector immediately before impact. The state vector of the robot immediately after the impact are then reset to

$$\begin{bmatrix} \boldsymbol{q}^{\mathrm{T}} \\ \dot{\boldsymbol{q}}^{\mathrm{T}} \end{bmatrix} = \begin{bmatrix} \theta_2 & \theta_1 & \theta_3 & \theta_6 & \theta_7 & \theta_4 & \theta_5 & x_1 & 0 \\ \dot{\theta}_2^+ & \dot{\theta}_1^+ & \dot{\theta}_3^+ & \dot{\theta}_6^+ & \dot{\theta}_7^+ & \dot{\theta}_4^+ & \dot{\theta}_5^+ & 0 & 0 \end{bmatrix}, \quad (15)$$

where the velocities with super script, "+", indicate those immediately after impact due to Eq. (14). Table I lists the mechanical parameters of the biped robot. We use these parameters in our simulations.

TABLE I
MECHANICAL PARAMETERS

Symbol	Unit	Value	Symbol	Unit	Value
m_1	kg	5.0	a_1	m	$l_1/2$
m_2	kg	5.0	a_2	m	$l_2/2$
m_3	kg	1.5	a_3	m	$l_3/2$
m_4	kg	1.5	a_4	m	$l_4/2$
m_h	kg	5.0	b_1	m	$l_1/2$
l_1	m	0.8	b_2	m	$l_2/2$
l_2	m	0.8	b_3	m	$l_3/2$
l_3	m	0.4	b_4	m	$l_4/2$
l_4	m	0.4	d_1	m	0.6
I_1	kg·m^2	$m_1 l_1^2/12$	I_2	kg·m^2	$m_2 l_2^2/12$
I_3	kg·m^2	$m_3 l_3^2/12$	I_4	kg·m^2	$m_4 l_4^2/12$

III. PRINCIPLE OF UP-AND-DOWN WOBBLING MASS

Here, we show the principle of an up-and-down wobbling mass for high-speed limit cycle walking [13]. Fig. 3 and Fig. 4 show the schematic illustration of the moment due to an up-and-down wobbling mass. We thus see that the reaction force due to the wobbling mass generates moment at the contact point of the stance-leg that is given by

$$\boldsymbol{M} = \boldsymbol{r} \times \boldsymbol{F}, \quad (16)$$

where $\boldsymbol{r}$ is the vector from the contact point to the hip joint and $\boldsymbol{F}$ is the reaction force vector due to the wobbling

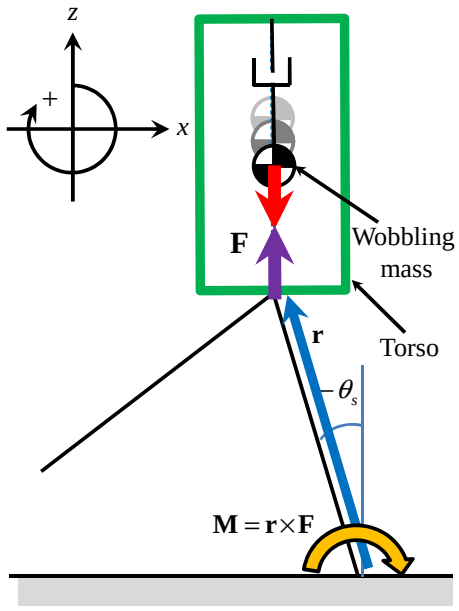

Fig. 3. Schematic illustration of moment due to wobbling mass at the negative stance leg angle

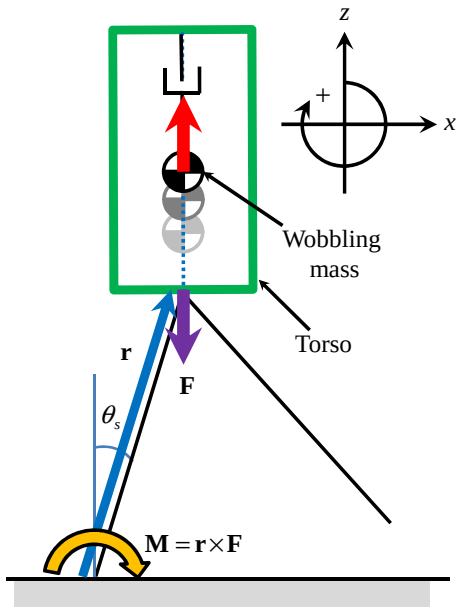

Fig. 4. Schematic illustration of moment due to wobbling mass at the positive stance leg angle

mass. Fig. 3 shows the moment when the wobbling mass is dropped at the negative stance leg angle. Then, Fig. 4 shows the moment when the wobbling mass is raised at the positive stance leg angle. We can see that biped walking speed increases by up-and-down of the wobbling mass based on the principle.

To achieve high-speed limit cycle walking, we design control method for biped robots with arms based on the principle.

IV. CONTROL METHODS

A. Swing-leg and torso control

We first show the control methods of the swing-leg and torso posture for level ground walking. We achieve level ground walking of the biped robot by using the following control methods:

$$u_1 = -K_{P1}(\theta_2 - \theta_1 - \phi_d) - K_{D1}(\dot{\theta}_2 - \dot{\theta}_1), \quad (17)$$

$$u_2 = -K_{P2}(\theta_3 - \theta_{3d}) - K_{D2}\dot{\theta}_3, \quad (18)$$

where K_{P1}, K_{P2}, K_{D1} and K_{D2} are the control gains, ϕ_d is the desire hip joint angle. The biped robot can achieve the desired hip-joint angle by Eq. (17) and the desired torso posture by Eq. (18).

B. Swing-arms control

We design control method for the swinging-arms based on the principle of the up-and-down wobbling mass. To generate the propulsive moment, biped robots drop the CoM (center of mass) of the arms when the stance leg angle is negative. Biped robots then raise the CoM of the arms to generate the propulsive moment when the stance leg angle is positive. These motions are given by

$$u_3 = -K_{P3}(\theta_4 - K_a\theta_1) - K_{D3}(\dot{\theta}_4 - K_a\dot{\theta}_1), \quad (19)$$

$$u_4 = -K_{P4}(\theta_5 - K_a\theta_1) - K_{D4}(\dot{\theta}_5 - K_a\dot{\theta}_1), \quad (20)$$

$$u_5 = -K_{P5}(\theta_6 + K_a\theta_1) - K_{D5}(\dot{\theta}_6 + K_a\dot{\theta}_1), \quad (21)$$

$$u_6 = -K_{P6}(\theta_7 + K_a\theta_1) - K_{D6}(\dot{\theta}_7 + K_a\dot{\theta}_1), \quad (22)$$

where K_{P3}, K_{P4}, K_{P5}, K_{P6}, K_{D3}, K_{D4}, K_{D5} and K_{D6} are the control gains and K_a is the control parameter for amplitude of swinging-arms. Table II lists the control parameters.

V. WALKING ANALYSIS

Fig. 5 shows the kinetic, potential and mechanical energy (KE, PE and ME) in limit cycle walking at $K_a = 1.0$. Fig. 6 show the torque in the limit cycle walking. We can see that the biped robot achieves periodic walking. Fig. 7 shows the stance leg angle and Height of the CoM of the arms from the mass point of the torso with respect to time. We see that the CoM of the arms goes up and down based on the principle of an up-and-down wobbling mass.

Fig. 8 shows the walking speed and Fig. 9 shows the specific resistance (SR) in limit cycle walking with respect

TABLE II
CONTROL PARAMETERS

Symbol	Value	Symbol	Value
K_{P1}	100	K_{D1}	10
K_{P2}	1000	K_{D2}	100
K_{P3}	600	K_{D3}	60
K_{P4}	600	K_{D4}	60
K_{P5}	600	K_{D5}	60
K_{P6}	600	K_{D6}	60
ϕ_d	-0.60 [rad]	θ_{3d}	0.00 [rad]

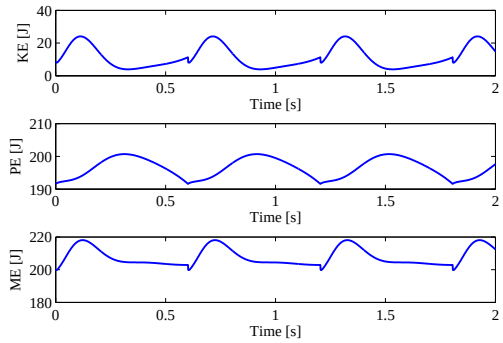

Fig. 5. Kinetic, potential and total mechanical energy with respect to time

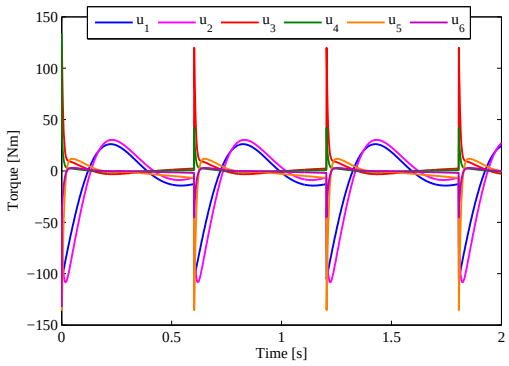

Fig. 6. Torque with respect to time

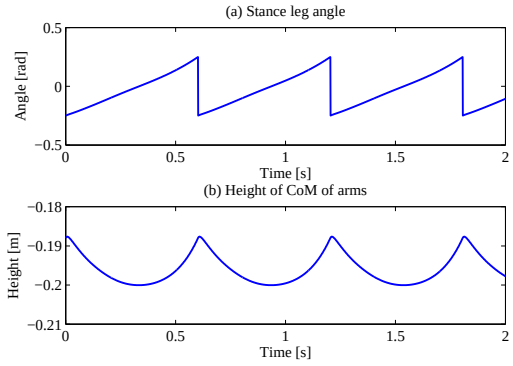

Fig. 7. Stance leg angle and height of CoM of arms from mass point of the torso with respect to time

to K_a. The SR is an index of energy-efficiency in dynamic walking given by

$$\mathrm{SR} := \frac{p}{Mgv}, \tag{23}$$

where p [J] is the average input power, M [kg] is the total weight of the robot and v [m/s] is the average walking speed. Average input power, p, is given by

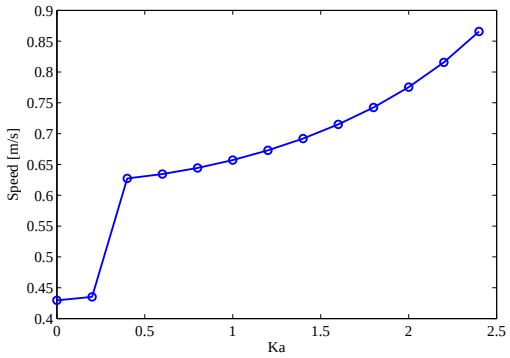

Fig. 8. Walking speed with respect to K_a

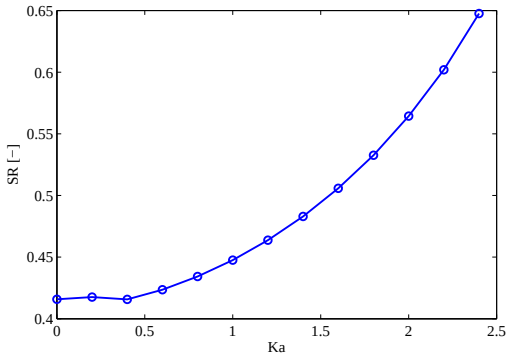

Fig. 9. SR with respect to K_a

$$p := \frac{1}{T}\int_0^T (|u_1(\dot{\theta}_2 - \dot{\theta}_3)| + |u_2(\dot{\theta}_3 - \dot{\theta}_1)| + |u_3(\dot{\theta}_4 - \dot{\theta}_3)| + |u_4(\dot{\theta}_5 - \dot{\theta}_4)| + |u_5(\dot{\theta}_6 - \dot{\theta}_3)| + |u_6(\dot{\theta}_7 - \dot{\theta}_6)|)dt, \tag{24}$$

where T [s] is the total walking time (n-steps).

We can see that walking speed and SR monotonically increases with respect to increasing K_a. Since K_a is the control parameter for amplitude of swinging arms, the amplitude of up-and-down CoM of the arms increase by increasing K_a. The waking speed thus increases and SR increases by the increasing impact effects due to the increasing walking speed. We can considerably improve walking speed of the biped robots by our proposed method. However, we cannot set overlarge K_a since biped robots have limit of motion range of the shoulder joints. we did not also use the elbow joint effectively for limit cycle walking yet. we expect that more high-speed walking by using the elbow joints. In the next section, we show a speeding-up method using the elbow joints effectively.

VI. WALKING ANALYSIS WITH BENDING ARMS

Fig. 10 shows schematic illustration of biped robot with bending arms. When the biped robot bend arms vertically at the elbow, the CoM of the arms generates the moment for

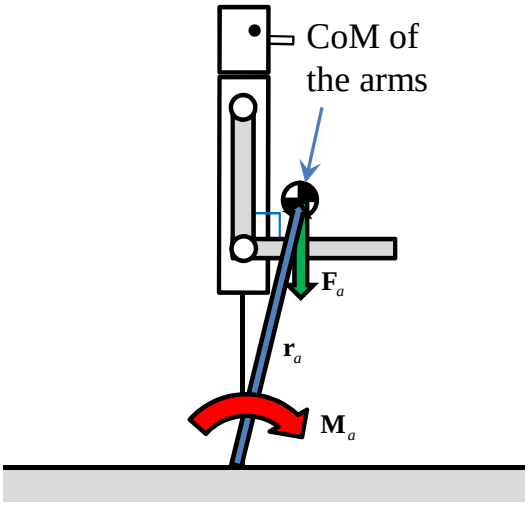

Fig. 10. Schematic illustration of biped robot with bending arms

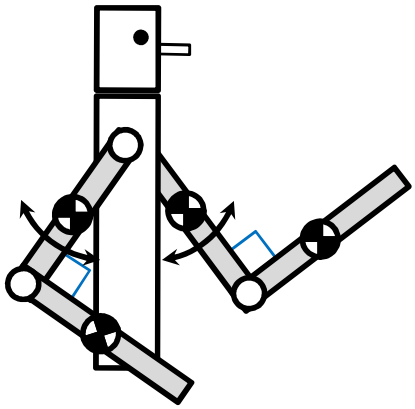

Fig. 11. Schematic illustration of swinging arms with bending arms

propulsive effect. The moment is given by

$$\boldsymbol{M}_a = \boldsymbol{r}_a \times \boldsymbol{F}_a, \tag{25}$$

where $\boldsymbol{r}_a$ is the vector from the contact point of the stance leg to the CoM of the arms and $\boldsymbol{F}_a$ is the force vector due to the CoM of the arms. We expect that biped robot achieves more high-speed walking by using swinging bending arms based on the principle of an up-and-down wobbling mass. We thus change two control method for swinging bending arms as shown in Fig. 11.

$$u_4 = -K_{P4}(\theta_5 - K_a\theta_1 + \pi/2) - K_{D4}(\dot{\theta}_5 - K_a\dot{\theta}_1), \tag{26}$$
$$u_6 = -K_{P6}(\theta_7 + K_a\theta_1 + \pi/2) - K_{D6}(\dot{\theta}_7 + K_a\dot{\theta}_1). \tag{27}$$

Fig. 12 shows the kinetic, potential and mechanical energy (KE, PE and ME) in limit cycle walking with bending arms at $K_a = 1.0$. Fig. 13 show the torque in the limit cycle walking. Fig. 14 shows the stance leg angle and height of the CoM of the arms from mass point of the torso with respect to time. We see that the biped robot achieves periodic walking and the CoM of the arms goes up and down based on the principle of an up-and-down wobbling mass.

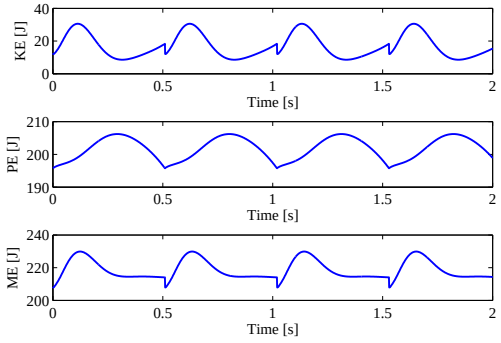

Fig. 12. Kinetic, potential and total mechanical energy with respect to time

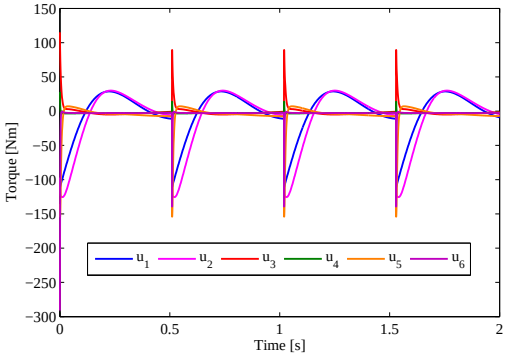

Fig. 13. Torque with respect to time

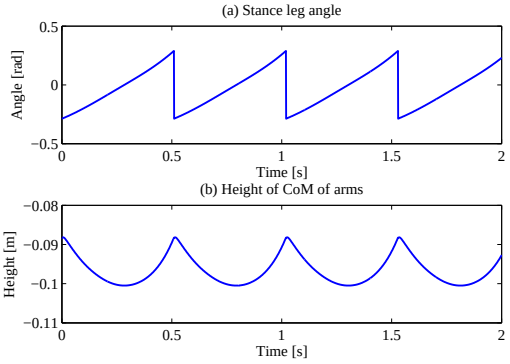

Fig. 14. Stance leg angle and height of CoM of arms from mass point of the torso with respect to time

Fig. 15 shows the walking speed of the limit cycle walking with respect to K_a. Fig. 16 shows the SR of the limit cycle walking with respect to K_a We see that walking speed and SR monotonically increase with respect to increasing K_a.

Fig. 17 shows comparison of waking speed between the biped robot with straight arms (Fig. 8) and the biped robot with bending arms (Fig. 15). We can see that the walking speed of the biped robot with bending arms is faster than that of the biped robot with straight arms. Fig. 18 shows comparison of SR between the biped robot with straight arms (Fig. 9) and the biped robot with bending arms (Fig. 16).

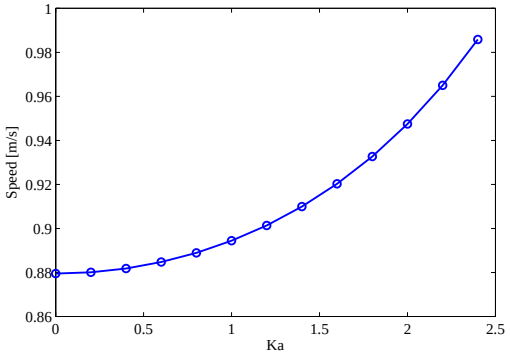

Fig. 15. Walking speed in bending arm with respect to K_a

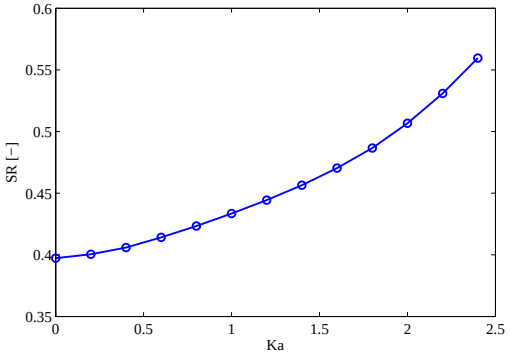

Fig. 16. SR in bending arm with respect to K_a

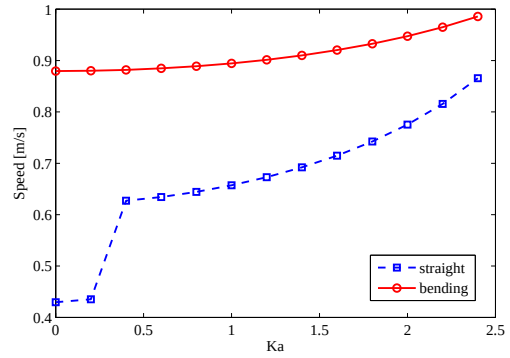

Fig. 17. Comparison of walking speed between biped robot with straight arms and biped robot with bending arms

From this figure, we see that the energy-efficiency of the biped robot with bending arms is better than that of the biped robot with straight arms. We thus see that swinging bending arms based on the principle of up-and-down wobbling mass is important for achieving high-speed limit cycle walking.

VII. CONCLUSION AND FUTURE WORK

In this paper, we presented a novel speeding-up method for biped walking using swinging-arms motion based on the principle of an up-and-down wobbling mass. we proposed a control method for swinging-arms motion based on the principle of up-and-down of a wobbling mass. By the proposed

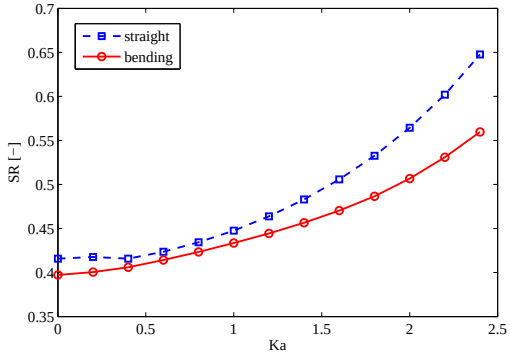

Fig. 18. Comparison of SR between biped robot with straight arms and biped robot with bending arms

method, the biped robot achieves high-speed limit cycle walking. Moreover, we have shown that the walking speed and energy-efficiency improve by using the bending arms. We plan to validate the our proposed method by experiment. Moreover, we want to extend our proposed method to 3D biped walking.

REFERENCES

[1] HONDA, "Humanoid Robot ASIMO," [Online]. Available: http://www.honda.co.jp/ASIMO/.

[2] PETMAN, "Boston dynamics: Humanoid robot petman," [Online]. Available : http://www.bostondynamics.com.

[3] AIST, "Humanoid robot hrp4-c," [Online]. Available : http://www.aist.go.jp.

[4] T. McGeer, "Passive dynamic walking," *The International Journal of Robotics Research*, vol. 9, no. 2, pp. 62–82, 1990.

[5] F. Asano, M. Yamakita, and K. Furuta, "Virtual passive dynamic walking and energy-based control laws," in *Proc. IEEE/RSJ International Conference on Intelligent Robots and Systems (IROS)*, 2002, pp. 1149–1154.

[6] M. Wisse and J. Van Frankenhuyzen, "Design and construction of mike; a 2d autonomous biped based on passive dynamic walking," in *Proc. International Symposium of Adaptive Motion and Animals and Machines (AMAM03)*, 2003.

[7] M. Wisse, "Three additions to passive dynamic walking; actuation, an upper body, and 3D stability," in *Proc. IEEE/RAS International Conference on Humanoid Robots (ICHR)*, vol. 1, 2004, pp. 113–132.

[8] D. G. E. Hobbelen and M. Wisse, "Limit cycle walking", *Humanoid Robots, Human-like Machines,* chapter 14. InTech, 2007.

[9] Y. Hanazawa, H. Suda, Y. Iemura, and M. Yamakita, "Active walking robot mimicking flat-footed passive dynamic walking," in *Proc. IEEE International Conference on Robotics and Biomimetics (ROBIO)*, 2012, pp. 1281–1286.

[10] F. Asano and Z. W. Luo, "Efficient dynamic bipedal walking using effects of semicircular feet," *Robotica*, vol. 29, no. 03, pp. 351–365, 2011.

[11] ——, "Energy-efficient and high-speed dynamic biped locomotion based on principle of parametric excitation," *IEEE Transactions on Robotics*, vol. 24, no. 6, pp. 1289–1301, 2008.

[12] D. Hobbelen and M. Wisse, "Controlling the walking speed in limit cycle walking," *The International Journal of Robotics Research*, vol. 27, no. 9, pp. 989–1005, 2008.

[13] Y. Hanazawa, T. Hayashi, M. Yamakita, and F. Asano, "High-speed limit cycle walking for biped robots using active up-and-down motion control of wobbling mass," in *Proc. IEEE/RSJ International Conference on Intelligent Robots and Systems (IROS)*, 2013, pp. 3649–3654.

[14] J. W. Grizzle, G. Abba, and F. Plestan, "Asymptotically stable walking for biped robots: Analysis via systems with impulse effects," *IEEE Transactions on Automatic Control*, vol. 46, no. 1, pp. 51–64, 2001.